

CLOPPA–IPPP Analysis of Cooperative Effects in Hydrogen-Bonded Molecular Complexes. Application to Intermolecular ${}^{2h}J(\text{N,C})$ Spin–Spin Coupling Constants in Linear $(\text{CNH})_n$ Complexes

Claudia G. Giribet* and Martín C. Ruiz de Azúa

Department of Physics, Facultad de Ciencias Exactas y Naturales, University of Buenos Aires, Ciudad Universitaria, Pab. I, (1428) Buenos Aires, Argentina

Received: December 27, 2007; In Final Form: February 18, 2008

The cooperative effects on NMR indirect nuclear coupling constants are analyzed by means of the IPPP–CLOPPA approach (where CLOPPA is the Contributions from Localized Orbitals within the Polarization Propagator Approach and IPPP is the Inner Projections of the Polarization Propagator). The decomposition of the J coupling allows one to classify these effects as those due to changes in the geometric structure and those that directly involve the transmission mechanisms. This latter contribution admits a further classification, taking into account its electronic origin. As an example, the cooperative effects on intermolecular ${}^{2h}J(\text{N,C})$ couplings of the linear complexes $(\text{CNH})_n$ ($n = 2, 3, 4$) are discussed.

Introduction

The influence of cooperative effects on molecular properties in hydrogen-bonded complexes has been the subject of widespread research, because of its great importance in biological, chemical, and physical systems. For example, it is well-known that these interactions play an important role in the stabilization and folding of molecules of biological interest.^{1–3} Although cooperative interactions in hydrogen-bonded assemblies are usually defined as the difference between the total interaction energy of the complex and the sum of pairwise interaction energies,^{4–6} many molecular properties are sensitive to this type of nonadditive effect, including, for example, dipole moments,^{7,8} molecular geometric conformations,^{4–6,8–12} vibrational stretching and bending frequencies,^{6,7,11} and NMR parameters such as chemical shifts^{9,12} and indirect nuclear spin–spin coupling constants.^{4,5,9–11,13–15} Several years ago, the electronic mechanisms operating on some of these properties were interpreted by means of an NBO analysis.⁷

The experimental detection of intermolecular spin–spin coupling constants between nuclei across hydrogen bonds has provided a powerful tool to identify and characterize hydrogen-bonded moieties. From their first measurement,^{16,17} extensive work has been done to study different aspects of this type of coupling, from a theoretical point of view.^{18–21} Because spin–spin couplings are very sensitive to structural changes, the analysis of the transmission mechanisms of intermolecular couplings can supply valuable information about cooperativity phenomena on hydrogen-bonded systems.

The CLOPPA (Contributions from Localized Orbitals within the Polarization Propagator Approach) method, combined with the IPPP (Inner Projections of the Polarization Propagator) technique,^{22–25} is a useful tool to identify the electronic mechanisms that are operating in a given phenomenon, in terms of localized molecular orbitals. It was implemented at the ab initio level for the theoretical analysis of NMR spin–spin couplings^{22–28} and the static molecular polarizability ten-

sor.^{26,27,29} This method was applied to study systems with hydrogen-bonded moieties (for instance, one-bond C–H couplings in complex systems with C–H···O interactions²⁹) and to determine the electronic mechanisms that result in ${}^{1h}J(\text{A,H})$ and ${}^{2h}J(\text{A,D})$ couplings across D–H···A hydrogen bonds in a set of small model compounds.³⁰ More recently, the method was also used to analyze the unusual behavior of the ${}^{2h}J(\text{F,F})$ coupling in the $(\text{HF})_2$ dimer, as a function of the hydrogen bond distance.³¹

The purpose of this work is to give a new insight on cooperative effects on NMR indirect spin–spin coupling constants in hydrogen-bonded complexes. The IPPP–CLOPPA decomposition of couplings in contributions from local fragments allows a suitable classification of cooperative interactions, according to their influence on different aspects of the coupling, and clarifies the electronic mechanisms that result in these effects. This approach complements the aforementioned studies, as the origin of these effects is analyzed in terms of localized molecular orbitals (LMOs) that closely represent chemical functions such as cores, bonds, lone pairs, and the corresponding antibonding orbitals. Transmission mechanisms are identified in terms of “coupling pathways” J_{ij} involving two occupied (i,j) localized molecular orbitals, and “coupling pathways” $J_{ia,jb}$ involving two occupied (i,j) and two vacant (a,b) LMOs. The relative importance of different LMOs and the role played by each one can then be assessed. It is noteworthy that, although the method is applied here for the analysis of cooperative effects on coupling constants, the same scheme can be used for any second-order molecular property.

The present paper is organized as follows. In first place, a brief account of the IPPP–CLOPPA method is presented. A classification of cooperative effects within the IPPP–CLOPPA method is presented for the first time. Numerical results of the IPPP–CLOPPA analysis of cooperative effects on ${}^{2h}J(\text{N,C})$ intermolecular couplings in the linear hydrogen-bonded complexes $(\text{CNH})_n$ ($n = 2, 3, 4$) are presented in the “Results and Discussion” section. As was previously reported,⁴ the ${}^{2h}J(\text{N,C})$ couplings in $(\text{CNH})_n$ complexes correlate very well with the corresponding couplings in the $(\text{NCH})_n$ series. However, the

* Author to whom correspondence should be addressed. E-mail: giribet@df.uba.ar.

former present larger values than the latter. This fact was attributed, at least partially, to an electron-transfer effect. This characteristic makes the intermolecular coupling ${}^{2h}J(N,C)$ in $(CNH)_n$ complexes an interesting and suitable example to show the potentialities of the method. Interesting features, which complement previous studies,^{4,7} are found.

Method

IPPP and CLOPPA Methods. The IPPP (Inner Projections of the Polarization Propagator approach) and the CLOPPA (Contributions from Localized Orbitals within the Polarization Propagator approach) methods have been described previously.^{22–25} For the sake of comprehension, their main ideas are briefly outlined. In what follows, the method is applied to the analysis of spin–spin coupling constants. However, it must be remembered that the same methodology can be applied to any second-order molecular property.

Within the polarization propagator (PP) formalism,³² any component of the spin–spin coupling constant between nuclei N and M can be expressed as²²

$$J(N,M) = \Omega \sum_{ia,jb} V_{ia}(N) P_{ia,jb} V_{jb}(M) \quad (1)$$

where Ω is a constant that is dependent on the interaction considered and contains, among other factors, the gyromagnetic factors of nuclei N and M; the i,j (a^*,b^*) indices represent occupied i,j (vacant a^*,b^*) molecular orbitals (MOs) of a Hartree–Fock (HF) reference state; $P_{ia,jb}$ is the PP matrix element that connects “virtual excitations” $i \rightarrow a^*$ and $j \rightarrow b^*$. $V_{ia}(N)$ represents the matrix element of the perturbative Hamiltonian between MOs i and a^* centered at nucleus N, and a similar definition exists for $V_{jb}(M)$. These elements are called “perturbators”.

In the IPPP–CLOPPA method, $J(N,M)$ (eq 1) is rewritten in terms of localized MOs (LMOs), by applying a convenient unitary transformation from canonical HF MOs to occupied and vacant LMOs to the PP matrix elements and to the perturbators, separately. These LMOs are obtained in such a way that they represent chemical functions such as bonds, lone pairs and atomic inner shells, and their corresponding “anti” LMOs (antibonds, anti-lone pairs, etc.). The localization technique used in this work is that which was reported by Engelmann,²² applied in an iterative way, as was described previously.^{30,31} The formal expression of $J(N,M)$, in terms of LMOs (eq 1) is not altered, but the indices i,j now represent occupied LMOs and the indices a,b represent vacant LMOs. $J(N,M)$ can be re-expressed in terms of four-indices “coupling pathways”, which involve two virtual excitations between occupied and virtual LMOs ($i \rightarrow a^*$ and $j \rightarrow b^*$):

$$J(N,M) = \sum_{ia,jb} J_{ia,jb} \quad (2)$$

where

$$J_{ia,jb} = \begin{cases} (V_{ia}(N)V_{jb}(M) + V_{jb}(N)V_{ia}(M))P_{ia,jb} & (\text{for } ia \neq jb) \\ V_{ia}(N)V_{jb}(M)P_{ia,jb} & (\text{for } ia = jb) \end{cases} \quad (3)$$

Within this approach, it is convenient to define two-indices contributions for a given pair of occupied LMOs i and j , by summing over the entire set of vacant LMOs. These contributions are dubbed “two-indices coupling pathways”:

$$J_{ij} = \sum_{a,b} J_{ia,jb} \quad (4)$$

As was shown in a previous paper,³⁰ in the particular case that the perturbative Hamiltonian is a Fermi contact-like (FC) operator, two-indices coupling pathways can be written as

$$J_{ij} \propto \frac{1}{2} \{ [|\tilde{\psi}_i^M(N)|^2 - |\psi_i(N)|^2] + [|\tilde{\psi}_j^M(N)|^2 - |\psi_j(N)|^2] \} \quad (5)$$

or, alternatively,

$$J_{ij} \propto \frac{1}{2} \{ [|\tilde{\psi}_i^M(N)|^2 - |\psi_i(N)|^2] + [|\tilde{\psi}_i^N(M)|^2 - |\psi_i(M)|^2] \} \quad (6)$$

where $|\psi_i(N)|^2$ is the electronic density of LMO i at the site of N nucleus, and $|\tilde{\psi}_i^M(N)|^2$ is the electronic density of the perturbed LMO i at the same site, due to the LMO j , perturbed at the M nucleus site, calculated up to second order, with regard to V . Equations 5 and 6 allow the following interpretation of two-indices coupling pathways J_{ij} :

(a) The sum of electronic density changes of LMOs i and j at the site of nucleus N when LMOs j and i are perturbed at the other nucleus, respectively.

(b) The sum of electronic density changes of LMO i at both nuclei sites when LMO j is perturbed at the other nucleus site.

Taking into account that, within ab initio calculations, there are several vacant LMOs that can be ascribed to each type of local fragment, four-indices coupling pathways are more conveniently defined as

$$J_{ia,jb} = \sum_{\substack{\alpha \in a^* \\ \beta \in b^*}} J_{\alpha i, \beta j} \quad (7)$$

where α (or β) represents vacant LMOs of the a^* (or b^*) type. These four-indices coupling pathways allow an interpretation that is similar to that of the two-indices coupling pathways. Again, as it was already demonstrated,³¹ these contributions can be re-expressed, up to second order in the perturbation, as

$$J_{ia,jb} \propto \frac{1}{2} \{ [|\tilde{\psi}_{ia}^M(N)|^2 - |\psi_i(N)|^2] + [|\tilde{\psi}_{jb}^M(N)|^2 - |\psi_j(N)|^2] \} \quad (8)$$

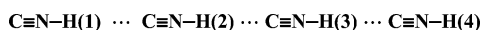
or, equivalently, as

$$J_{ia,jb} \propto \frac{1}{2} \{ [|\tilde{\psi}_{ia}^M(N)|^2 - |\psi_i(N)|^2] + [|\tilde{\psi}_{ia}^N(M)|^2 - |\psi_i(M)|^2] \} \quad (9)$$

where $\tilde{\psi}_{ia}^M(N)$ is the contribution to the perturbed LMO i at the site of nucleus N from the a^* -type vacant LMOs, due to LMO j connected to the vacant LMOs of the b^* -type by the FC perturbation at the site of nucleus M, and $\psi_i(N)$ is LMO i evaluated at the site of nucleus N.

The last two equations lead to the following interpretations of $J_{ia,jb}$:

(a) The sum of the contribution of the a^* -type vacant LMOs to the electronic density changes of LMO i and the contribution of the b^* -type vacant LMOs to LMO j at the site of one nucleus when LMOs j and i are connected to b^* -type and a^* -type vacant LMOs, respectively, at the other nucleus.

CHART 1: Labeling of the Molecules in the (CNH)_n (n = 2, 3, 4) Complexes

(b) The sum of the contribution of the a^* -type vacant LMOs to the electronic density changes of LMO i at both nuclei sites when LMO j is connected to b^* -type vacant LMOs at the other nucleus site.

It is noteworthy that, for long-range couplings, because of the local character of LMOs, only one electronic density change contributes significantly to the J_{ij} terms in eqs 5 and 6, and to the $J_{ia,jb}$ terms in eqs 8 and 9. Therefore, the sign and magnitude of these two- and four-indices coupling pathways can be determined by comparing the electronic density of a single perturbed LMO to that of the unperturbed LMO at a particular nucleus site.

Within the present implementation, the IPPP–CLOPPA analysis can be performed only at the RPA level.

Local Contributions. The contribution to the coupling constant transmitted through a certain molecular fragment S (which could be the entire molecule) is obtained by restricting the sum of eq 2 to the subset of LMOs that define S. This type of contribution is called the “CLOPPA contribution”:

$$J^S(\text{N},\text{M}) = \sum_{ia,jb \in S} J_{ia,jb} = \Omega \sum_{ia,jb \in S} V_{ia}(\text{N}) P_{ia,jb} V_{jb}(\text{M}) \quad (10)$$

Although i,a^* , j,b^* are the only LMOs to appear explicitly in each of the four-indices coupling pathways, it must be emphasized that the influence of the other spin-polarized LMOs is also present through the PP matrix element $P_{ia,jb}$. Hence, if the contribution to the coupling transmitted strictly through a fragment S that is defined by a subset of occupied and vacant LMOs is sought ($J^{L(S)}$), it can be defined using the IPPP technique as^{10–13}

$$J^{L(S)}(\text{N},\text{M}) = \sum_{ia,jb \in S} J^{L(S)}_{ia,jb} = \Omega \sum_{ia,jb \in S} V_{ia}(\text{N}) W_{ia,jb} V_{jb}(\text{M}) \quad (11)$$

where $J^{L(S)}_{ia,jb}$ is calculated as described by eq 3 but now the PP element is obtained by inner-projecting the full PP matrix on the set of virtual excitations among LMOs within the molecular fragment S ($W_{ia,jb}$). In this way, electrons that do not belong to the molecular fragment S are not allowed to be spin-polarized, neither by direct interaction with the nuclei nor by Coulomb interactions with the polarized electrons in S. $J^{L(S)}$ is dubbed the “local” contribution to the coupling transmitted through the fragment S (or the IPPP contribution). The contribution that is transmitted by the remainder of the molecule (J^R) can be determined as follows:

$$J^R = J - J^{L(S)} \quad (12)$$

Finally, the indirect influence of the other LMOs, which do not belong to S, on coupling pathways within S, can be estimated as follows:

$$J^S_{\text{ind}} = \sum_{ia \geq jb \in S} J_{ia,jb} - J^{L(S)}_{ia,jb} \quad (13)$$

where the first term of eq 13 is calculated with the full PP matrix. It is noteworthy that, because the perturbators in each term of the sum in eq 13 are the same, this quantity describes how much LMOs other than those that belong to S contribute

to define the magnitude of the PP matrix elements that are associated with virtual excitations within S.

Classification of Cooperative Effects within the IPPP–CLOPPA Method. Cooperative interactions affect molecular properties through several mechanisms that, despite their shared electronic origin, can be classified depending on their influence on different aspects of the molecular property. Thus, a first classification of cooperative effects on a certain property can distinguish between effects due to changes in the geometric structure and effects that directly involve the transmission mechanisms. In the case discussed in the present work of the intermolecular coupling constants in hydrogen-bonded complexes (CNH)_n, the following separation can hold:

$$J_n(\text{N},\text{M}) = J_{2,\text{sim}}(\text{N},\text{M}) + \Delta J_G + \Delta J_T \quad (14)$$

where $J_n(\text{N},\text{M})$ is the coupling constant in (CNH)_n and $J_{2,\text{sim}}(\text{N},\text{M})$ is the same coupling constant in the dimer ($n = 2$), but built in such a way that both monomers have the same geometric structure. The latter coupling is considered to be a reference and is dubbed $J_{\text{ref}}(\text{N},\text{M})$ (that is, without cooperative effects). ΔJ_G is the contribution to the coupling due to geometric cooperative effects (“geometric effects G”):

$$\Delta J_G = J_n(\text{N},\text{M}) - J_{n,\text{sim}}(\text{N},\text{M}) \quad (15)$$

where $J_{n,\text{sim}}(\text{N},\text{M})$ corresponds to the n -complex in which all monomers have the same unrelaxed geometric structure. ΔJ_T is the contribution to the coupling due to effects that directly involve transmission mechanisms (“transmission effects T”). This latter contribution admits a further classification, taking into account its origin:

$$\Delta J_T = \Delta J_D + \Delta J_I + \Delta J_\Psi \quad (16)$$

where ΔJ_D is the contribution due to virtual excitations that involve LMOs of the local fragment S and at least one of the rest of the complex.

$$\Delta J_D = J_{n,\text{sim}}(\text{N},\text{M}) - J^S_{n,\text{sim}}(\text{N},\text{M}) \quad (17)$$

The local fragment S, in this case, is spanned by the subset of LMOs that belong to both monomers involved in the coupling. It can be dubbed the “direct effect D”. Following the notation of eq 10, $J^S_{n,\text{sim}}(\text{N},\text{M})$ is calculated as a CLOPPA contribution onto the local fragment S.

The second term, ΔJ_I ,

$$\Delta J_I = J^S_{n,\text{sim}}(\text{N},\text{M}) - J^{L(S)}_{n,\text{sim}}(\text{N},\text{M}) \quad (18)$$

takes into account the indirect influence of the remainder of the complex on the coupling transmission and it can be called the “indirect effect I”. $J^{L(S)}_{n,\text{sim}}(\text{N},\text{M})$ is the “strictly local contribution”, which is calculated using the IPPP technique (eq 11). The transmission of this term is mediated by electronic interactions between local and nonlocal fragments, which are taken into account in the PP matrix elements.

The third term of eq 16, ΔJ_Ψ ,

$$\Delta J_\Psi = J^{L(S)}_{n,\text{sim}}(\text{N},\text{M}) - J_{\text{ref}}(\text{N},\text{M}) \quad (19)$$

takes into account the changes in the LMOs of the local fragment that are due to the contribution of the nonlocal fragment. It will be called the “molecular effect M”.

Taking into account all effects, the intermolecular coupling constant can be expressed as

$$J_n(N,M) = J_{\text{ref}}(N,M) + \Delta J_G + \Delta J_D + \Delta J_I + \Delta J_\Psi \quad (20)$$

Finally, each cooperative contribution to a particular two-indices coupling pathway can be also determined, following eq 5, as follows:

$$\Delta J_{D,ij} \propto [|\tilde{\psi}_i^M(N)|_{\text{tot}}|^2 - |\tilde{\psi}_i^M(N)|_S|^2] \quad (21)$$

$$\Delta J_{I,ij} \propto [|\tilde{\psi}_i^M(N)|_S|^2 - |\tilde{\psi}_i^M(N)|_{L(S)}|^2] \quad (22)$$

$$\Delta J_{\Psi,ij} \propto [|\tilde{\psi}_i^M(N)|_{L(S)}|^2 - |\tilde{\psi}_i^M(N)|_{\text{ref}}|^2] - [|\tilde{\psi}_i^M(N)|_{L(S)}|^2 - |\tilde{\psi}_i^M(N)|_{\text{ref}}|^2] \quad (23)$$

where the notation used is the same as that used in eq 5, and sub-indices indicate the subspace of vacant LMOs contributions to the perturbed or unperturbed LMO. Thus, the subscript “tot” means that all vacant LMOs are considered, the subscripts “S” and “L(S)” respectively correspond to having a CLOPPA or IPPP calculation, and the subscript “ref” indicates the perturbed or unperturbed LMO of the reference dimer.

Results and Discussion

To illustrate the preceding discussion, cooperative effects on the ${}^{2h}J(N,C)$ intermolecular coupling constant in the linear hydrogen-bonded complexes $(\text{CNH})_n$ ($n = 2, 3, 4$) are analyzed. Calculations were performed at the RPA level, using the SYSMO program.^{33–35} CLOPPA and IPPP analysis of the J couplings were performed using a modified version of the SYSMO program. Only Fermi contact (FC) terms are considered, because it has been shown that this contribution is most affected by cooperative effects.⁴ The atomic orbital basis set used is that of Van Duijneveldt³⁶ (13s7p1d,8s1p)–[13s5p1d,5s1p]. Geometrical structures, optimized at the MP2³⁷ level using cc-pVTZ-J³⁸ basis sets, were taken from ref 4. The “symmetric” complexes were constructed using the optimized geometric structure of the first monomer of $(\text{CNH})_2$. The numbering of the monomers within the complexes is shown in Chart 1. To facilitate the comparison between similar couplings in different complexes, the following notation is used. J_1 refers to ${}^{2h}J(N,C)$ between the first two terminal monomers (1 and 2 in all complexes), J_2 is the same coupling between intermediate inner monomers (2 and 3 in $(\text{CNH})_4$), and J_3 is the coupling between the last two terminal monomers (2 and 3 in $(\text{CNH})_3$, and 3 and 4 in $(\text{CNH})_4$). Finally, the notation used to identify occupied and vacant LMOs is depicted in Table 1.

The localization procedure was extensively explained previously;^{30,31} therefore, only a few comments are pertinent here. As determined previously,^{30,31} several vacant LMOs are localized in the hydrogen-bond regions N–H...C. These types of LMOs are called “bridge vacant LMOs” (σ or π). It is noteworthy that this type of LMOs arises from canonical MOs with low orbital energies. This fact, as was remarked previously,^{30,31} indicates that they are physically significant in the complex formation. There are also a few (one for the trimer and two for the tetramer) vacant LMOs completely delocalized over the entire complex. They present peaks that are centered in C atom sites, similar to “anti lone pairs”. Finally, it is worth mentioning that vacant LMOs that belong to each monomer were combined in a sole group, as the influence of each monomer on the others is sought.

In Table 2, total values of ${}^{2h}J(N,C)$ for all complexes for both optimized and symmetric geometries are displayed. SOPPA values taken from ref 4 are also shown for comparison. This

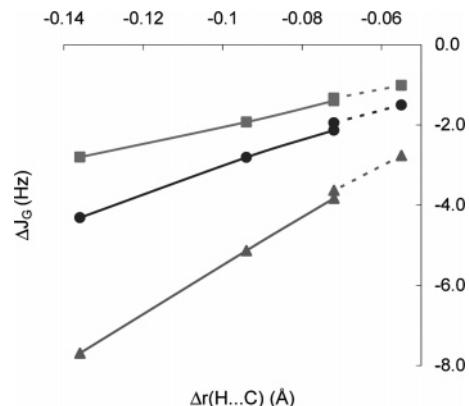


Figure 1. Geometric (G) cooperative effect on main two indices coupling pathways and total coupling constants versus the change in the hydrogen bond distance: (●) C–N(2)/LP(1), (■) C–N(2)/C–N(2), and (▲) total coupling. Solid lines correspond to the $(\text{CNH})_4$ complex, and dashed lines correspond to the $(\text{CNH})_3$ complex.

TABLE 1: Labeling of the LMOs

| | occupied LMOs | vacant LMOs |
|--|----------------|----------------------------|
| (anti)inner shell of atom X | S(X) | S(X)* |
| σ -(anti)bond between X and Y | X–Y | X–Y* |
| π -(anti)bond | π_x, π_z | π_x^*, π_z^* |
| (anti) lone pair of atom X | LP | LP* |
| vacant LMOs belonging to monomers n and m ($n, m = 1-4$) | | CN _{<i>n,m</i>} * |
| σ -bridge vacant LMOs ($n = 1-3$) | | HB _{<i>n</i>} * |
| π -bridge vacant LMOs ($n = 1-3$) | | HB π_n^* |
| delocalized vacant LMOs | | noI* |

table shows that, although correlation effects are not negligible, RPA values follow the same trends as SOPPA values. In fact, although overestimated, the relative values among all couplings are well-reproduced by RPA values, in comparison with SOPPA ones. These results strongly suggest that no triplet instability is associated with the π electronic system. This assertion was further verified in two ways. On one hand, a RPA–IPPP calculation of the π transmitted contribution to the coupling in, for instance, the $(\text{CNH})_2$ dimer, yields -2.73 Hz. On the other hand, multiconfigurational self-consistent field (MCSCF) calculations were performed at the complete active space (CAS) level for the $(\text{CNH})_2$ dimer. These calculations were performed by means of the Dalton program.³⁹ In the first case, all 8 π electrons were allowed to correlate, considering the π^* vacant MOs of lowest orbital energy. In the second case, all 8 π electrons and 8 σ electrons distributed on 14 active MOs (8 π MOs and 6 σ MOs) were considered. The obtained values (-19.50 and -18.39 Hz, respectively) confirm that there is no triplet instability problem associated with the spin–spin couplings analyzed in this work. Therefore, it can be concluded that RPA values are adequate for performing a qualitative analysis of cooperative effects in these intermolecular couplings.

In Table 3, geometric and transmission cooperative effects are shown, which have been calculated following eqs 15 and 16. This table shows that all cooperative effects are negative; consequently, all couplings are larger (in absolute value) for the trimer and the tetramer complex than for the dimer. Geometric (G) cooperative effects are more important than transmission (T) effects. However, the latter are also significant. It is interesting to observe that G effects seem to be strongly dependent on both the position within the chain of the units involved and the total length of the chain, whereas T effects are dependent mainly on the former. However, as will be seen in the next section, the dependence of the G effect can be mainly

TABLE 2: Total Values of ${}^{2h}J(\text{N,C})$ for All Complexes for Both Optimized and Symmetric Geometric Structures^a

| | $J(\text{N1,C2})$ | | | $J(\text{N2,C3})$ | | | $J(\text{N3,C4})$ | | |
|--------------------|---------------------|---------------------|--------------------|---------------------|---------------------|--------------------|---------------------|---------------------|--------------------|
| | RPA ^b | | SOPPA ^c | RPA ^b | | SOPPA ^c | RPA ^b | | SOPPA ^c |
| | optimized structure | symmetric structure | | optimized structure | symmetric structure | | optimized structure | symmetric structure | |
| (CNH) ₂ | -20.28 | -20.33 | -16.3 | | | | | | |
| (CNH) ₃ | -23.91 | -21.15 | -19.2 | -25.5 | -21.87 | -20.5 | | | |
| (CNH) ₄ | -25.22 | -21.39 | -20.3 | -30.48 | -22.79 | -24.5 | -27.33 | -22.2 | -22.0 |

^a All values given in units of Hz. See Chart 1 for numeration. ^b Corresponding to RPA values with either an optimized geometric structure or a “symmetric” geometric structure. ^c Corresponding to SOPPA values with optimized geometric structure (taken from ref 4).

TABLE 3: Geometric and Transmission Cooperative Effects in ${}^{2h}J(\text{N,C})$ for All Complexes Considered^a

| | $J1$ | | | $J2$ | | | $J3$ | | |
|--------------------|----------------|----------------|-------|----------------|----------------|--------|----------------|----------------|-------|
| | G ^b | T ^c | total | G ^b | T ^c | total | G ^b | T ^c | total |
| (CNH) ₂ | 0.05 | | 0.05 | | | | | | |
| (CNH) ₃ | -2.76 | -0.83 | -3.50 | | | | -3.63 | -1.55 | -5.18 |
| (CNH) ₄ | -3.83 | -1.07 | -4.90 | -7.69 | -2.47 | -10.16 | -5.13 | -1.88 | -7.01 |

^a All values given in units of Hz. See text for definitions of $J1$, $J2$, and $J3$. ^b G refers to geometric cooperative effects. ^c T refers to transmission cooperative effects.

TABLE 4: Transmission Cooperative Effects, Classified According to Their Origin^a

| | D ^b | I ^c | M ^d | total |
|--------------------|----------------|----------------|----------------|-------|
| | | $J1$ | | |
| (CNH) ₃ | 0.68 | -0.69 | -0.81 | -0.83 |
| (CNH) ₄ | 0.83 | -1.24 | -0.65 | -1.07 |
| | | $J2$ | | |
| (CNH) ₄ | -0.86 | -0.85 | -0.75 | -2.47 |
| | | $J3$ | | |
| (CNH) ₃ | -4.77 | 0.41 | 2.82 | -1.55 |
| (CNH) ₄ | -4.6 | 0.49 | 2.24 | -1.88 |

^a All values given in units of Hz. ^b See eq 17. ^c See eq 18. ^d See eq 19.

ascribed to only one geometric parameter change, namely, the change in the length of the hydrogen bond involved in the coupling. Both types of effects are maximum for $J2$ (that is, for the coupling between the two inner monomers), whereas the effects on $J1$ are the smallest effects.

Finally, T effects can be further classified following eqs 16–19. Table 4 presents the values obtained. It is interesting to observe that the large negative direct effect in $J3$ is partially compensated by the molecular one, which is quite large and positive. For $J2$, the total relevant effect is due to the sum of very small negative components. $J1$ generally presents small terms. The analysis of the electronic mechanisms that originate these cooperative effects is performed using the IPPP–CLOPPA approach, taking into account two-indices (J_{ij}) coupling pathways and the four-indices ($J_{ia,jb}$) coupling pathways.

Two-Indices ${}^{2h}J_{ij}(\text{N,C})$ and Four-Indices ${}^{2h}J_{ia,jb}(\text{N,C})$ Contributions to Cooperative Effects. Figure 1 depicts the dependence of the geometric (G) cooperative effects on total couplings and main two-indices (J_{ij}) terms, C–N(2)/LP(1) and C–N(2)/C–N(2), as a function of the change in the length of the hydrogen bond between the optimized geometric structures and the symmetric ones ($\Delta r(\text{H}\dots\text{C})$). The number 1 (or 2) given in the brackets indicates that the LMO belongs to the first (or second) coupled unit, and “LP” indicates the lone pair of the nitrogen atom.

It is noteworthy that the geometric effect on the two-indices terms C–N(2)/LP(1) and C–N(2)/C–N(2) and on the total couplings follows an almost-linear dependence on $\Delta r(\text{H}\dots\text{C})$, regardless of the complex or the position of the units involved in the coupling. However, the small gap that can be observed

between the coupling values that correspond to the (CNH)₄ and (CNH)₃ complexes shows that the geometric effect is also affected by the different electronic surroundings, but only slightly. The linear dependence can be justified as follows. In the C–N(2)/C–N(2) term, both LMOs involved belong to only one of the molecules. Thus, an exponential decrease (in absolute value) could be expected for this type of terms, because their contributions are dependent on the “tails” of occupied C–N(2) at the N(1) nucleus. On the other hand, in the C–N(2)/LP(1) term, the distance dependence is determined by the interaction (mostly electrostatic) between C–N(2) and LP(1). Therefore, an inverse power decrease (in absolute value) could be expected for this type of term. This functional dependence is not fully observed in Figure 1; instead, a first-order expansion of both exponential and potential functions is observed, as the range of distances considered is very small. It is also interesting to note that the geometric effect is larger in a term such as C–N(2)/LP(1) than in C–N(2)/C–N(2). However, the percentage of change is quite similar in both types of terms.

The transmission (T) cooperative effects on the two-indices coupling pathways are depicted in Table 5. Total, CLOPPA, and IPPP values are also given and compared to the reference values (${}^{2h}J_{2,\text{sim}}(\text{N,C})$) in the dimer. Several comments in this table are pertinent. Only two coupling pathways—the two main ones, which practically dominate the entire coupling—exhibit important influences by T effects. These are, again, LP(1)/C–N(2) and C–N(2)/C–N(2). Other terms, such as LP(1)/N–H(1), are also affected by this type of effect, but to a much lesser extent. It is noteworthy that cooperative effects are only due to vacant LMOs. Occupied LMOs are not involved in cooperative effects at all, which can be realized by considering that two-indices coupling pathways that involve one or two occupied LMOs of nonlocal units give negligible contributions. Each type of transmission effect deserves the following analysis.

The direct contribution arises from four-indices coupling pathways in which some indices belong to the local subspace while the others belong to the nonlocal subspace. This contribution has a large value for $J3$ and $J2$, mainly because of the LP(1)/C–N(2) term, whereas it is rather small for $J1$ (for example, in (CNH)₄, -4.51 Hz for $J3$, -2.63 Hz for $J2$, and -0.17 Hz for $J1$). This indicates that the latter coupling is originated only in the local subspace (it must be taken into account that there is no significant four-indices coupling pathways that mix virtual excitations from both local and

TABLE 5: Transmission Cooperative Effects on the Main Two-Indices Coupling Pathways (Total, CLOPPA, and IPPP Values, in Comparison with Reference Values, Are Also Given)

| | | reference | total | CLOPPA | IPPP | T-Cooperative Effects | | | total |
|--------------------|--------|-----------------------|--------|--------|--------|-----------------------|----------------|----------------|-------|
| | | | | | | D ^b | I ^c | M ^d | |
| | | ^{2h} J1(N,C) | | | | | | | |
| (CNH) ₃ | | -20.33 | -21.15 | -21.83 | -21.14 | 0.68 | -0.69 | -0.81 | -0.82 |
| LP(1) | C-N(2) | -11.60 | -12.1 | -12.31 | -11.92 | 0.21 | -0.39 | -0.32 | -0.50 |
| C-N(2) | C-N(2) | -7.41 | -7.86 | -8.12 | -7.76 | 0.26 | -0.36 | -0.35 | -0.45 |
| LP(1) | N-H(1) | -2.35 | -2.35 | -2.50 | -2.33 | 0.15 | -0.17 | 0.02 | 0.00 |
| (CNH) ₄ | | -20.33 | -21.39 | -22.22 | -20.98 | 0.83 | -1.24 | -0.65 | -1.06 |
| LP(1) | C-N(2) | -11.60 | -12.23 | -12.54 | -11.84 | -0.17 | -0.70 | -0.24 | -1.11 |
| C-N(2) | C-N(2) | -7.41 | -7.98 | -8.34 | -7.88 | 0.36 | -0.46 | -0.47 | -0.57 |
| LP(1) | N-H(1) | -2.35 | -2.36 | -2.51 | -2.32 | 0.15 | -0.19 | 0.03 | -0.01 |
| | | ^{2h} J2(N,C) | | | | | | | |
| (CNH) ₄ | | -20.33 | -22.79 | -21.93 | -21.08 | -0.86 | -0.85 | -0.75 | -2.46 |
| LP(1) | C-N(2) | -11.60 | -13.03 | -10.40 | -11.40 | -2.63 | 1.00 | 0.20 | -1.43 |
| C-N(2) | C-N(2) | -7.41 | -8.58 | -8.54 | -8.14 | -0.04 | -0.40 | -0.73 | -1.17 |
| LP(1) | N-H(1) | -2.35 | -2.38 | -2.99 | -2.24 | 0.61 | -0.75 | 0.11 | -0.03 |
| | | ^{2h} J3(N,C) | | | | | | | |
| (CNH) ₃ | | -20.33 | -21.87 | -17.10 | -17.51 | -4.77 | 0.41 | 2.82 | -1.54 |
| LP(1) | C-N(2) | -11.60 | -12.47 | -7.78 | -8.87 | -4.69 | 1.09 | 2.73 | -0.87 |
| C-N(2) | C-N(2) | -7.41 | -8.07 | -6.35 | -6.81 | -1.72 | 0.46 | 0.60 | -0.66 |
| LP(1) | N-H(1) | -2.35 | -2.37 | -2.31 | -2.02 | -0.06 | -0.29 | 0.33 | -0.02 |
| (CNH) ₄ | | -20.33 | -22.20 | -17.60 | -18.09 | -4.60 | 0.49 | 2.24 | -1.87 |
| LP(1) | C-N(2) | -11.60 | -12.65 | -8.14 | -9.35 | -4.51 | 1.21 | 2.25 | -1.05 |
| C-N(2) | C-N(2) | -7.41 | -8.22 | -6.53 | -7.00 | -1.69 | 0.47 | 0.41 | -0.81 |
| LP(1) | N-H(1) | -2.35 | -2.38 | -2.33 | -2.11 | -0.05 | -0.22 | 0.24 | -0.03 |

^a All values given in units of Hz. Numbers between brackets in LMO names indicate that the LMO belongs to first (1) or second (2) coupled units. ^b See eq 17. ^c See eq 18. ^d See eq 19.

nonlocal fragments), whereas a considerable contribution for *J*₂ and *J*₃ arises from the nonlocal subspace. To understand the reason of this different behavior, the LP(1)/C-N(2) term is analyzed by means of eq 21. Figures 2a-c graphically show the direct effect on this term, by means of the difference $|\tilde{\psi}_i^M|_{\text{tot}}^2 - |\tilde{\psi}_i^M|_S^2$, where $\tilde{\psi}_i^M$ represents the perturbed LMO C-N(2) due to the LMO LP(1) perturbed at the M=N(1) nucleus in (CNH)₄, the subscript "tot" indicates that the contribution of all vacant LMOs is taken into account, and the subscript "S" refers to the contribution of the CN12* vacant LMOs (Figure 2a), the CN23* vacant LMOs (Figure 2b), and the CN34* vacant LMOs (Figure 2c), for both perturbed LP(1) and C-N(2) LMOs.

The different amount of the direct effect, depending on the intermolecular coupling considered, can be explained as follows. As was mentioned previously, the electronic density difference $|\tilde{\psi}_i^M|_{\text{tot}}^2 - |\tilde{\psi}_i^M|_S^2$ evaluated at the C(2) nucleus site for perturbed C-N(2) LMO shows the magnitude of the direct effect on the coupling considered. This change of density when the C-N(2) LMO is allowed to mix (i) with all vacant orbitals (totally perturbed LMO) or (ii) only with those of the CN12* type (locally perturbed LMO) can be considered to be the response of the C-N(2) LMO due to the magnetic perturbation of LP(1) at the N(1) nucleus, because this LMO is also allowed to connect with the same vacant orbitals depicted in situations (i) and (ii). It must be taken into account that, when a given LMO is magnetically perturbed and allowed to connect with vacant LMOs, the distribution of electronic charge within the molecule is altered. As a result, the mean electric field acting on other LMOs is changed. This internal change is described by the polarization propagator. When a dominant mechanism operates, this change can be explained on qualitative grounds. Thus, in that sense, the direct effect on the LP(1)/C-N(2) term is dependent on to which vacant orbitals the perturbed LP(1) LMO are allowed to connect in both situations and how much spread becomes in each case. For the case depicted in Figure 2a (*J*₁), the perturbed lone pair LP(N1) can mix only with vacant

orbitals of the CN12* type, mainly with HB1*. Thus, the totally perturbed LP(N1) would be practically the same as the locally perturbed one. As a consequence, it can be expected that the perturbed C-N2 orbital does not significantly change its density at the C2 site when it can mix with all vacant orbitals or only with those of the CN12* type. Therefore, the direct effect on *J*₁ coupling is very small. On the contrary, for the case depicted in Figure 2c (*J*₃), the perturbed LP(N3) LMO can be connected not only to CN34* vacant orbitals but also with CN23* vacant orbitals (mainly with those of the HB2* type). Consequently, the electric field generated by the perturbed LP(N3) LMO is less local when this LMO is allowed to connect with all vacant LMOs than when it is restricted to be mixed only with CN34* vacant LMOs. Therefore, it can be expected that the former field favors the electronic charge flow toward the CNH(3) zone more than the latter. Consequently, the totally perturbed C-N4 LMO decreases its density in the CNH(4) zone, with respect to the locally perturbed one, and, thus, the direct effect are significant. A similar analysis can be made for the case depicted in Figure 2b (*J*₂), and, hence, similar conclusions hold. It is interesting to observe that, by inspection of the four-indices coupling pathways, there are only two types of nonlocal vacant LMOs that are responsible of the direct effect: the "bridge" vacant LMOs of the σ type (HB_{*n*}*), and the delocalized vacant LMOs. For example, by including these types of LMOs in the calculation of ^{2h}*J*₃(N,C) in (CNH)₃, the CLOPPA calculation changes from -17.60 Hz to -21.55 Hz (cf. total value: -21.87 Hz). In other words, the direct cooperative effect is mainly due to virtual excitations from two local occupied LMOs (LP(1) and C-N(2)) to these two nonlocal types of vacant LMOs.

Generally, smaller contributions than the preceding ones are due to the indirect effect, as can be observed from Table 5. However, it is relevant to note that this slight, but non-negligible, effect is mainly due to the nonlocal "bridge" vacant LMOs of the σ and π types (HB_{*n*}* and HB π_n *) and the delocalized vacant LMOs. Actually, if these vacant LMOs are included in the IPPP calculation, the IPPP results match those of the CLOPPA

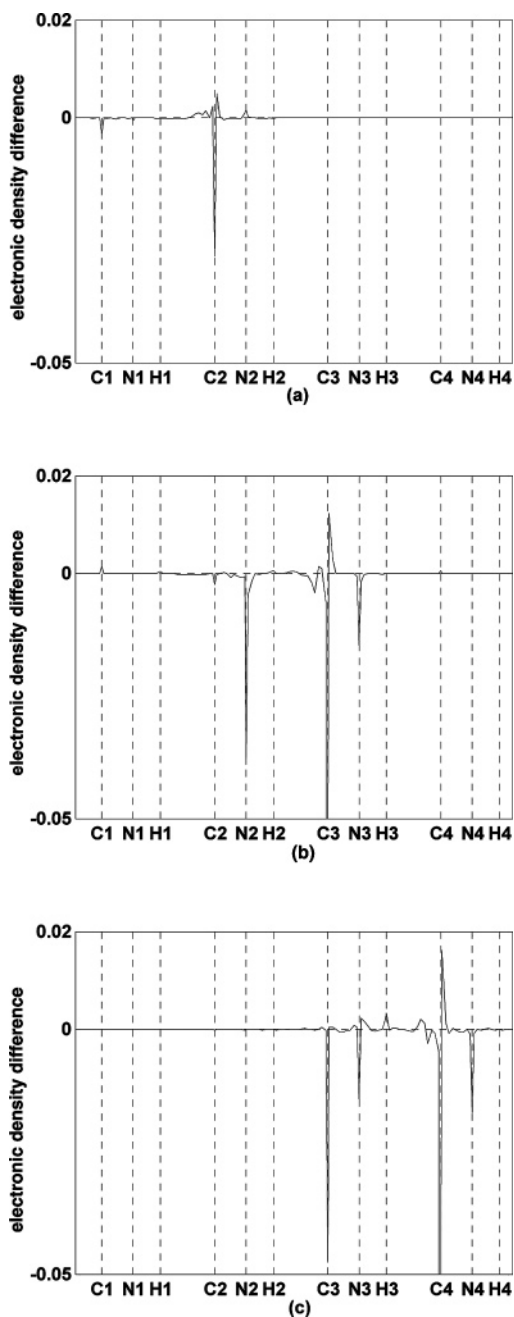


Figure 2. Graphical representation of the direct effect (given in units of a.u.) on the LP(1)/C–N(2) term of intermolecular coupling constants in (CNH)₄, by means of eq 21: (a) J_1 , (b) J_2 , and (c) J_3 .

calculation in Table 5. This fact shows that the indirect effect is mainly mediated by the spin polarization of local electrons to this type of nonlocal vacant LMOs.

Finally, the molecular effect is due to the contribution of the nonlocal atomic centers to the local LMOs. In this case, this effect is only important for the LP(1)/C–N(2) term of J_3 , in both (CNH)₃ and (CNH)₄ complexes, and it is positive, thus contributing to decrease the coupling. It is noteworthy that, despite this latter term, in all the other terms, the “totally local” contribution almost matches the reference value.

Concluding Remarks

The IPPP–CLOPPA decomposition of NMR indirect spin–spin couplings in contributions of local fragments is shown to lead to a suitable classification of cooperative interactions, according to their influence on different aspects of the coupling.

Although one must remember that these effects have a common electronic origin, they can be primarily classified as effects that are due to changes in the geometric structure (geometric effects) and effects that directly involve transmission mechanisms (transmission effects). The latter can be further decomposed in those effects due to (a) the direct influence of the nonlocal molecular fragment, i.e., the subspace spanned by LMOs that do not involve the coupled nuclei (direct effects); (b) the indirect influence of the nonlocal fragment, through electronic interactions between the local and nonlocal subspaces included in the PP matrix elements (indirect effects); and (c) the changes in the local LMOs due to the contribution of the nonlocal fragment (molecular effects). The analysis of cooperative effects on intermolecular ${}^2hJ(\text{N,C})$ couplings of the linear complexes (CNH)_{*n*}, presented as a suitable example, shows the potentialities of the method. The use of LMOs allows a discussion of cooperative mechanisms, in terms of a few main two- and four-indices coupling pathways. Geometric effects are dependent, almost exclusively, on the change in the length of the hydrogen bond. Direct transmission effects can be rationalized in terms of the electronic density difference, at the coupled nucleus site, of the perturbed LMO involved when (a) the contribution of all vacant LMOs of the molecule is taken into account, and (b) only local vacant LMOs are considered. Indirect effects are shown to be due only to the spin polarization of local electrons to a few nonlocal vacant LMOs, the σ and π “bridge” vacant LMOs, and the completely delocalized vacant LMOs. Finally, it is shown that all these cooperative effects are only attributable to vacant LMOs.

Acknowledgment. Financial support from UBACYT and CONICET is gratefully acknowledged. We would like to thank Prof. P. Lazzarotti for providing us a copy of the SYSMO program.

References and Notes

- (1) Gu, J.; Wang, J.; Leszczynski, J. *J. Phys. Chem. B* **2004**, *108*, 8017.
- (2) Koch, O.; Bocola, M.; Klebe, G. *Proteins: Struct. Funct. Bioinf.* **2005**, *61*, 310.
- (3) Fernández, A.; Rogale, K. *J. Phys. A* **2004**, *37*, L197.
- (4) Provasi, P. F.; Aucar, G. A.; Sánchez, M.; Alkorta, I.; Elguero, J.; Sauer, S. P. A. *J. Phys. Chem. A* **2005**, *109*, 6555.
- (5) van Mourik, T.; Dingley, A. J. *J. Phys. Chem. A* **2007**, *111*, 11350.
- (6) Parra, R. D.; Gong, B.; Zeng, X. C. *J. Chem. Phys.* **2001**, *115*, 6036.
- (7) King, B. F.; Weinhold, F. *J. Chem. Phys.* **1995**, *103*, 333.
- (8) Znamenskiy, V. S.; Green, M. E. *J. Chem. Theory Comput.* **2007**, *3*, 103.
- (9) Tolstoy, P. M.; Schah-Mohammadi, P.; Smirnov, S. N.; Golubev, N. S.; Denisov, G. S.; Limbach, H. H. *J. Am. Chem. Soc.* **2004**, *126*, 5621.
- (10) Çarçabal, P.; Jockusch, R. A.; Hünig, I.; Snoek, L. C.; Kroemer, R. T.; Davis, B. G.; Gamblin, D. P.; Compagnon, I.; Oomens, J.; Simons, J. P. *J. Am. Chem. Soc.* **2005**, *127*, 11414.
- (11) Masella, M.; Flament, J. P. *J. Chem. Phys.* **1998**, *108*, 7141.
- (12) Ludwig, R.; Weinhold, F.; Farrar, T. C. *J. Phys. Chem. A* **1997**, *101*, 8861.
- (13) Juranić, N.; Macura, S. *J. Am. Chem. Soc.* **2001**, *123*, 4099.
- (14) Juranić, N.; Moncrieffe, M. C.; Likić, V. A.; Prendergast, F. G.; Macura, S. *J. Am. Chem. Soc.* **2002**, *124*, 14221.
- (15) Salvador, P.; Kobko, N.; Wieczorek, R.; Dannenberg, J. J. *J. Am. Chem. Soc.* **2004**, *126*, 14190.
- (16) Rae, I. D.; Weigold, J. A.; Contreras, R. H.; Biekofsky, R. R. *Magn. Reson. Chem.* **1993**, *31*, 836.
- (17) (a) Dingley, A. J.; Grzesiek, S. *J. Am. Chem. Soc.* **1998**, *120*, 8293. (b) Dingley, A. J.; Masse, J. E.; Peterson, R. D.; Barfield, M.; Feigon, J.; Grzesiek, S. *J. Am. Chem. Soc.* **1999**, *121*, 6019.
- (18) Fukui, H.; Baba, T. In *Specialist Periodical Reports: Nuclear Magnetic Resonance*; Royal Society of Chemistry: London, 2000; Vol. 30, p 109 (and references cited therein).
- (19) Kamienska-Trela, K.; Wojcik, J. In *Specialist Periodical Reports: Nuclear Magnetic Resonance*; Royal Society of Chemistry: London, 2002; Vol. 32, p 181 (and references cited therein).

- (20) Alkorta, I.; Elguero, J. *Int. J. Mol. Sci.* **2003**, *4*, 64 (and references cited therein).
- (21) Kamienska-Trela, K.; Wojcik, J. In *Specialist Periodical Reports: Nuclear Magnetic Resonance*; Royal Society of Chemistry: London, 2005; Vol. 34, p 196 (and references cited therein).
- (22) Engelmann, A. R.; Contreras, R. H. *Int. J. Quantum Chem.* **1983**, *23*, 1033.
- (23) Ruiz de Azúa, M. C.; Diz, A. C.; Giribet, C. G.; Contreras, R. H.; Rae, I. D. *Int. J. Quantum Chem.* **1986**, *S20*, 585.
- (24) Diz, A. C.; Giribet, C. G.; Ruiz de Azúa, M. C.; Contreras, R. H. *Int. J. Quantum Chem.* **1990**, *37*, 663.
- (25) Ruiz de Azúa, M. C.; Giribet, C. G.; Vizioli, C. V.; Contreras, R. H. *J. Mol. Struct. (THEOCHEM)* **1998**, *433*, 141.
- (26) Giribet, C. G.; Ruiz de Azúa, M. C.; Gómez, S. B.; Botek, E. L.; Contreras, R. H.; Adcock, W.; Della, E. W.; Krstic, A. R.; Lochert, I. J. *J. Comput. Chem.* **1998**, *19*, 181.
- (27) Giribet, C. G.; Demarco, M. D.; Ruiz de Azúa, M. C.; Contreras, R. H. *Mol. Phys.* **1997**, *91*, 105.
- (28) Lazzeretti, P.; Malagoli, M.; Zanasi, R.; Della, E. W.; Lochert, I. J.; Giribet, C. G.; Ruiz de Azúa, M. C.; Contreras, R. H. *J. Chem. Soc. Faraday Trans.* **1998**, *91*, 4031.
- (29) Giribet, C. G.; Ruiz de Azúa, M. C.; Vizioli, C. V.; Cavasotto, C. N. *Int. J. Mol. Sci.* **2003**, *4*, 203.
- (30) Giribet, C. G.; Ruiz de Azúa, M. C. *J. Phys. Chem. A* **2005**, *109*, 11980.
- (31) Giribet, C. G.; Ruiz de Azúa, M. C. *J. Phys. Chem. A* **2006**, *110*, 11575.
- (32) Jørgensen, P.; Simons, J. *Second Quantization-based Methods in Quantum Chemistry*; Academic Press: London, 1981.
- (33) Lazzeretti, P.; Zanasi, R. *J. Chem. Phys.* **1982**, *77*, 2448.
- (34) Lazzeretti, P. *Int. J. Quantum Chem.* **1979**, *15*, 181.
- (35) Lazzeretti, P. *J. Chem. Phys.* **1979**, *71*, 2514.
- (36) Van Duijneveldt, F. B. *IBM Res. Rep.* **1971**, RJ 945.
- (37) Møller, C.; Plesset, M. S. *Phys. Rev.* **1934**, *46*, 618.
- (38) Dunning, T. H., Jr. *J. Chem. Phys.* **1989**, *90*, 1007.
- (39) Helgaker, T.; Aa. Jensen, H. J.; Jørgensen, P.; Olsen, J.; Ruud, K.; Ågren, H.; Auer, A. A.; Bak, K. L.; Bakken, V.; Christiansen, O.; Coriani, S.; Dahle, P.; Dalskov, E. K.; Enevoldsen, T.; Fernandez, B.; Hättig, C.; Hald, K.; Halkier, A.; Heiberg, H.; Hetttema, H.; Jonsson, D.; Kirpekar, S.; Kobayashi, R.; Koch, H.; Mikkelsen, K. V.; Norman, P.; Packer, M. J.; Pedersen, T. B.; Ruden, T. A.; Sanchez, A.; Saue, T.; Sauer, S. P. A.; Schimmelpfennig, B.; Sylvester-Hvid, K. O.; Taylor, P. R.; Vahtras, O. DALTON, A Molecular Electronic Structure Program, Release 1.2, 2001.